1 **Climatic characteristics of the Jianghuai cyclone and its linkage with**

2 **precipitation during the Meiyu period from 1961 to 2020**

3 Ran Zhu[1], Lei Chen[1,2]

4 [1]Department of Atmospheric Science, School of Environmental Studies, China University of

5 Geosciences, Wuhan, 430074, China

6 [2]Centre for Severe Weather and Climate and Hydro-Geological Hazards, Wuhan, 430074, China

7 Correspondence to: Lei Chen (leichen@cug.edu.cn)

8 **Abstract.** This study examines the climatic characteristics of 202 Jianghuai cyclones

9 and their linkage with precipitation during the Meiyu period from 1961 to 2020. The

10 results show that cyclones mainly originate from eastern Hubei Province and south-

11 central Anhui Province, and further explore the statistical characteristics of the strength,

12 radius, and their positive correlation. When studying the decadal variation of cyclones,

13 we find that there is a similar trend between the decadal variation of cyclones and Meiyu

14 precipitation. Therefore, we further investigate the correlation between the Jianghuai

15 cyclones and the precipitation during the Meiyu period. There is a positive correlation

16 coefficient of 0.77 between them. It's worth mentioning that the percentage of

17 precipitation affected by cyclone activities can reach up to 47%. The anomalous

18 increase in precipitation caused by cyclones above 27°N can reach a maximum of 7

19 mm/day. When the cyclone existed, there was a significant altitude anomaly of negative

20 geopotential height can be traced to day -4 at the 500 hPa level over Mongolia. The

21 abnormally enhanced WPSH, southwesterly low-level jet and negative geopotential

22 height are the dominant factors causing abnormal precipitation during Jianghuai

23 cyclones. Before and after the cyclone developed, water vapor flux and divergence from

24 low latitudes abnormally increased. These provide sufficient water vapor conditions for

25 the generation of cyclone precipitation.

## 1. Introduction

Meiyu is a special rainy season due to the progress of the East Asian summer monsoon. The East Asian summer monsoon broke out in the South China Sea in mid-May and then advanced northward, forming rain bands in South China, the Jianghuai region, the Korean Peninsula and Japan (Ding et al., 2004,2007; Qian et al., 2000). The name for this special rainy season is called Meiyu in China, while it is called Changma in South Korea and it is called Baiu in Japan (Ninomiya et al., 1987; Oh et al., 1997; Saito. 1995). Meiyu front is one of the important weather systems affecting summer precipitation in the middle and lower reaches of the Yangtze River (Pang et al., 2013; Tao et al., 1979; Wang et al., 2014; Zhou et al., 2022). From mid-June to early July, the east of Yichang, Hubei Province, has continuous rains and short sunshine. These conditions are accompanied by heavy rainfall, strong wind and other weather phenomena in these areas during the Meiyu period (Ding. 1992; Zhao et al., 2021; Zhou et al., 2017). In China, the mean annual precipitation during the Meiyu period in the Jianghuai River Basin can reach 300 mm, accounting for 30%-40% of the mean annual total precipitation, and even up to 500 mm or more in the extreme Meiyu period (Liu et al., 2020). Historically, most of the summer floods disasters are caused by precipitation anomalies in the Meiyu period. Some scholars have studied and analyzed the representative floods of 1996, 1998, 2016 and 2020 (Bao et al., 2021; Su et al., 2021; Zhao et al., 2018; Zhong et al., 2023). These floods, caused by the Meiyu front, had adverse effects on people's safety, lives and property (Yan et al., 2021). Scholars in China have divided rainstorms caused by Meiyu fronts into three types (Zhang et al., 2004). The first type is the β mesoscale convective rainstorm on the Meiyu front. This type of rainstorm has a range of less than 300 km with strong intensity and a fast formation process (He et al., 2007). It is difficult to forecast before 12 hours and can be detected only by using radar to make a proximity forecast (Zhang et al., 2002). The second type is the persistent rainstorm located in front of the upper trough of low pressure in the western part of the Meiyu front. It is characterized by a long duration of approximately 5 days but appears less frequently, mainly in western Hubei and western

Hunan and Sichuan (Cai et al., 2021; Wu et al., 2020a;). The last type is the rainstorm caused by the Jianghuai cyclone located east of the origin of the Meiyu. The Jianghuai cyclones are affected by the thermal conditions of the sea and land and likely occur in the eastern part of the Meiyu front (Wang et al., 2016). The positive vorticity advection in front of the high-altitude trough and the warm advection in front of the front promote the eastward movement and development of the cyclone (Shen et al., 2019; Zhang et al., 2016). During the development of the cyclone, the lower levels are dominated by the southwest warm and humid airflow, and the high levels are mainly affected by dry and cold air (Zhao et al., 2008). This type of rainstorm has a large range, high intensity and long duration of precipitation (Wang et al., 2012; Xu et al., 2011).

Scholars' studies on Jianghuai cyclones during the Meiyu period were initially based on individual case analysis. Xu et al. (2013) studied a cyclone process in 2011 and found that the cyclone process lasted up to 36 h. The cyclone rainstorm was distributed on the south side of the cyclone. Heavy precipitation during the whole cyclone mainly occurred in the lower reaches of the Yangtze River. Wu et al. (2020b) studied 2 different cyclone rainstorm processes. They found that rainfall is directly proportional to cyclone intensity. There is a strong convergence center of water vapor flux during cyclone development. Zhou et al. (2020) found that a tornado was generated from the cyclone occlusion stage on July 22. The tornado was under the influence of a strong and fast Jianghuai cyclone and produced heavy precipitation accompanied by thunderstorm phenomena. With the improvement of cyclone identification methods and reconstruction of reanalysis data, statistical studies of cyclones have been further developed (Simmonds et al., 1999; 2000; Wernli et al., 2006). Yang et al. (2010) modeled the rainstorm process in the lower reaches of the Yangtze River from 1998 to 2005. The cyclones accounted for 62.5% of the rainstorm cases, and more than 70% of the cyclones could develop and produce rainstorms. The Jianghuai cyclone located in the lower reaches of the Yangtze River generally exists in the lower troposphere at 700 hPa. The horizontal scale is within 400 km, and the life period on land is generally less than 48 h. Wang et al. (2015) found that the number of cyclones was lower and their

intensity was weak in the 1980s and 1990s. In the early 2000s, cyclones were more frequent, and their intensity increased. After 2010, there was again a decreasing trend. Zhang et al. (2018) divided 60 cases of extreme precipitation in the middle reaches of the Yangtze River from 2008 to 2015 into five types. Among them, the extreme precipitation of the Jianghuai cyclone type accounted for 30%. The stable and maintained Western Pacific subtropical high (WPSH) system is one of the important reasons for the strong precipitation produced by cyclones. Because of the weak cold air force, the intensity of the Jianghuai cyclone is weaker than that in spring (Zhou et al., 2017). The daily analysis of the Jianghuai cyclones in the Meiyu period is easy to ignore. All these studies indicate that the Jianghuai cyclone is an important weather system that causes heavy rainfall during the Meiyu period in the middle and lower reaches of the Yangtze River (Wu et al., 2021; Zhang et al., 2018; Zhu et al., 1998).

Research on the climatic characteristics and precipitation effects of Jianghuai cyclones during the Meiyu period in the past 60 years has not yielded clear results. In this study, the relative vorticity method is used to objectively identify and track cyclones based on reanalysis data provided by ERA5. The climatological characteristics of the Jianghuai cyclones during this period are studied. We analyze the correlation between Jianghuai cyclone activity and precipitation. This study provides a reference for the long-term and short-term forecasting of precipitation in the Meiyu period.

The remainder of the present paper is organized as follows. Section 2 of this paper presents the dataset and analytical methods. In Section 3, we show the climatology composite of the cyclone tracks, genesis locations, intensity, lifetime and so on. There is a positive correlation between the frequency of cyclonic activity and precipitation in the Meiyu period. The relationship between them is studied by means of the geopotential height anomaly and water vapor flux anomaly. Section 4 provides the main discussion and findings of this study.

110
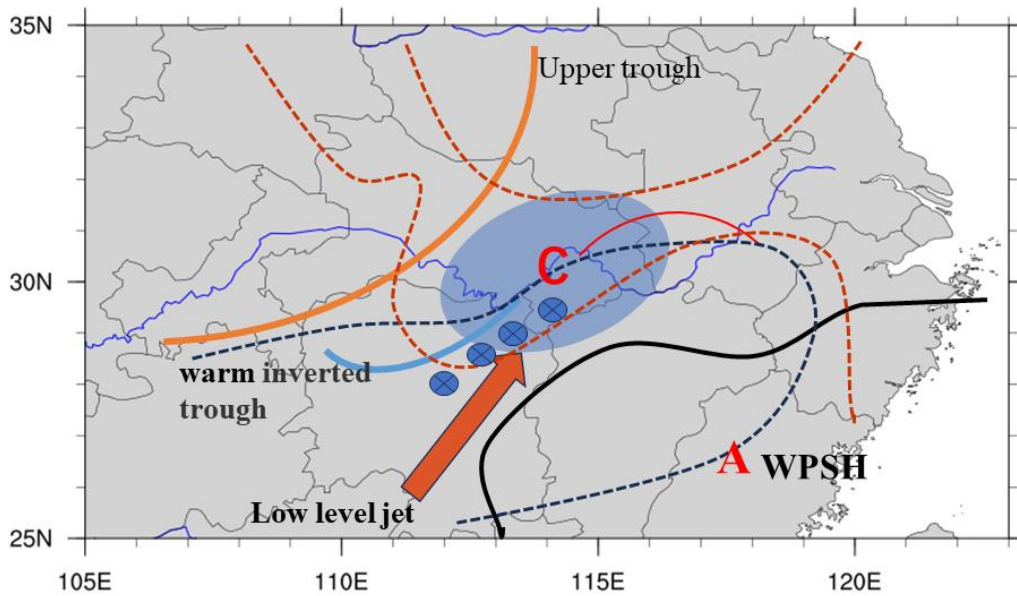
Fig.1 Schematic diagram of the main weather system and the structure of temperature and pressure field in the middle and low levels of the Jianghuai cyclone. (Red dotted line: isotherm; Solid black line: contour line; Blue dot: precipitation area; Solid orange line: 500 hPa upper-level trough; Red arrow: low level jet; Black dotted line: warm inverted trough; Solid red line: warm shear; Solid blue line: cold shear; Letter C: cyclone; Letter A: WSPH.)

## 2. Data and methods

### 2.1 Data

The time span of all the data is 60 years from 1961 to 2020, and the study area is located at 108°E-123°E, 27°N-34°N. We use the ERA5 relative vorticity hourly data (850 hPa) released by the European Centre for Medium Range Weather Forecasts (ECMWF) for Jianghuai cyclone identification and tracking. The spatial resolution of the data is 0.25°×0.25°, and the temporal resolution is 6 h. Every 6 h was defined as a step. The data of geopotential height, wind field, and specific humidity are daily data processed from ERA5 hourly data with a spatial resolution of 0.25°×0.25° (Hersbach et al., 2018). The geopotential height and wind field data include pressure levels of approximately 500 hPa, 700 hPa and 850 hPa. The specific humidity data include

128  pressure levels of approximately 500 hPa, 700 hPa and 850 hPa. The precipitation data

129  are from the CN05.1 grid point observation dataset compiled by the National

130  Meteorological Information Center of China Meteorological Administration with a

131  resolution of 0.25°×0.25° (Wu et al., 2013; Xu et al., 2009).

132  We used the Meiyu intensity index to characterize the strength of Meiyu, and data

133  is from the National Climate Center of China. The area for which the Meiyu intensity

134  index is calculated is defined in the article (GB/T 33671-2017). The Meiyu intensity

135  index is defined as:

136
$$M = \frac{L}{L_0} + \frac{0.5(R/L)}{R_0/L_0} + \frac{R}{R_0} - 2.5$$

137  M is the Meiyu intensity index. L is the length of the Meiyu in a given year (unit:

138  day) and $L_0$ means the average length of the Meiyu over the years (units: day). R is the

139  total precipitation of Jianghuai River basin during Meiyu in a given year, and $R_0$ is the

140  average total precipitation of Jianghuai River basin during Meiyu over the years. The

141  average period is from 1961 to the current year. For example, $L_0$ and $R_0$ values for 2000

142  are the averages from 1961 to 2000. Where M between -0.375 and 0.375, China

143  Meteorological Administration defines this year as the normal. Where M between 0.375

144  and1.25, this year is defined as a little strong. Where M greater than or equal to 1.25,

145  this year is defined as strong. Where M between -1.25 and -0.375, this year is defined

146  as a little weak. Where M less than or equal to -1.25, this year is defined as weak.

147  **2.2 Methods**

148  Scholars have proposed a number of methods to identify extratropical cyclones.

149  The objective identification and tracking method for cyclones used in this paper is the

150  vorticity tracking method proposed by Hodges (1994, 1995). This method mainly uses

151  the relative vorticity field at the 850 hPa to determine the feature points of the cyclone.

152  Feature points are used to correspond to the position of the cyclone and to match the

153  cyclone track within a given time span. In addition to the relative vorticity method of

154  tracking proposed by Hodges, different methods of cyclone identification have also

155  been proposed by other scholars. Lu (2017) improved the extratropical cyclone

identification and tracking method involving the nine-point pressure minimum. Jiang et al. (2020) proposed an algorithm for identifying extratropical cyclones on the basis of gridded data. This algorithm is named the eight-section slope detection method.

Among them, the most commonly used cyclone tracking methods are the mean sea level pressure method (SLP) and 850 hPa relative vorticity method. Mailier et.al (2006) and Zhang et.al (2012) studied the tracks of individual cyclones in these two methods. Both of them found 850 hPa relative vorticity method can identify and detect cyclone center earlier than the SLP method (Mailier et al., 2006). The reason for this result is that SLP is easily affected by topography and large-scale background circulation shear vorticity (Hodges, 1994). So based on this advantage of the relative vorticity method, we select the 850 hPa relative vorticity tracking method. The relative vorticity tracking method can detect low vortex systems earlier and track cyclones for a longer period of time with better stability. When the closed pressure levels are not visible on the satellite map, the vorticity tracking method can still continue to track the cyclone, improving the accuracy of cyclone track data.

## 3. Results

**3.1 Climatic characteristics of the Jianghuai cyclone during the Meiyu period**

A total of 202 Jianghuai cyclones existed during the Meiyu period from 1961 to 2020. The range of cyclone genesis locations defined by the Jiangsu Meteorological Administration (2017) and the characteristics of the relative vorticity tracking method were used. We adjust the genesis location and remove the cyclones that are generated at sea and have no effect on land precipitation (108°E-123°E, 28°N-35°N). To explore the tracks and genesis location of Jianghuai cyclone, we make a statistical of them (Fig.2). The brown dots represent the genesis locations, the first place meeting the criterion, of the Jianghuai cyclone. The yellow lines indicate the tracks of the cyclones. As shown in the figure, most of the cyclones develop in the Jianghan Plain and southern Anhui Province, then move eastward to the Yellow Sea coast. Some cyclones move northward through Shandong Province and reach the Bohai Sea. These tracks are

184 related to the upper-level guide airflow of 500~700 hPa. They are also affected by the

185 WPSH and its southwest warm and moist air on the edge (Wei et al., 2013).

186     Figure 2b shows the frequency of cyclone occurrence refers to the total number

187 of cyclones during the Meiyu period from 1961 to 2020.The genesis locations of

188 cyclones are mainly located in the middle and lower reaches of the Yangtze River and

189 the Huaihe River basin, with an east–west band distribution (Wang et al., 2015; Wu et

190 al., 2021). The frequency of occurrence refers to the total number of cyclones during

191 the Meiyu period from 1961 to 2020 is higher in the region of the Western Hubei

192 Province and Eastern Hubei Province. Research has found that the genesis locations of

193 cyclones are closely related to the topography (Xu 2021; Zhang et al., 2012).
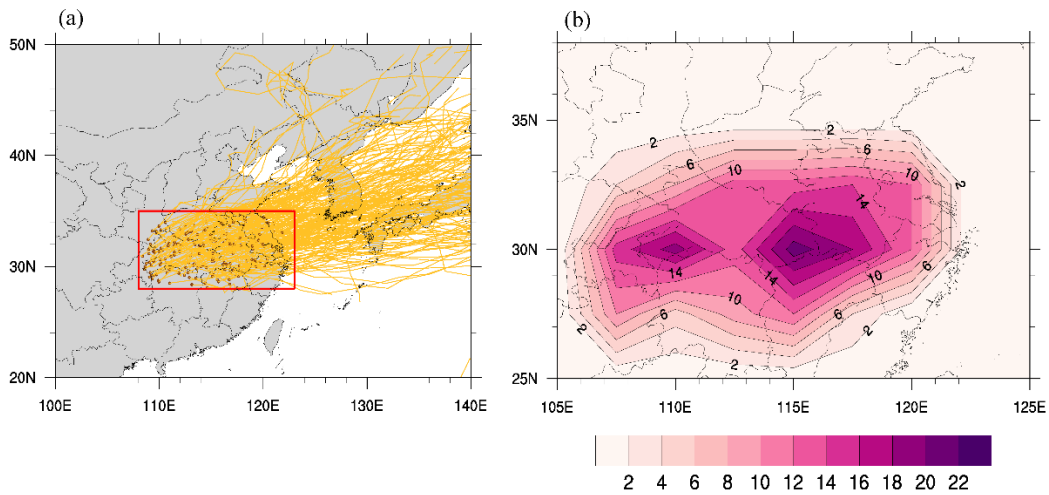
194 Fig 2. Distribution of the cyclone genesis locations, tracks (a) and the frequency of

195 genesis locations refers to the total number of cyclones (b) during the Meiyu period

196 from 1961 to 2020.

197     To examine the climatological characteristics of Jianghuai cyclones over 60 years,

198 we focus on the intensity, radius, and lifetime of cyclones on land. The intensity of the

199 Jianghuai cyclone is defined as the relative vorticity intensity of the 850 hPa cyclone

200 center. The lifetime is defined as the time of cyclones affecting precipitation on land.

201 Figure 3a shows that among the 202 selected cyclones, the intensity of the cyclone

202 center mainly ranges from $1.5 \times 10^{-5}$ s$^{-1}$ to $7.3 \times 10^{-5}$ s$^{-1}$. The number of cyclones in the

203 range of $2 \times 10^{-5}$ s$^{-1}$ to $3 \times 10^{-5}$ s$^{-1}$ has the largest proportion, accounting for 36% of the

total number of cyclones. A total of 180 cyclones are in the range of $1.5\times10^{-5}\,s^{-1}$ to $5\times10^{-5}\,s^{-1}$ in intensity, accounting for 89%. Figure 3b shows the relationship between the radius of cyclones and the number of cyclones. Most of the cyclones have an average radius between 300 and 800 km, accounting for 96% of the total number. The number of cyclones with radii between 500 and 600 km is the largest, accounting for 35%. Figure 3c shows the relationship between the time of cyclones affecting precipitation on land and the number of cyclones. Most of the cyclones affect precipitation on land for 1-3 days, and only one cyclone affects precipitation on land for more than 3 days. The number of cyclones' lifetime that affected precipitation on land within 2 days was 186, accounting for 92% of the total number.

The intensity of cyclone is one of the factors affecting its precipitation and impact range during the Meiyu period (Zhao et al., 2010). Figure 4a shows a positive correlation between the maximum intensity and the maximum radius of cyclone development. Therefore, the horizontal scale of most strong cyclones is larger than that of weak cyclones, the precipitation is greater, and the precipitation range is larger. From the distribution of difference value of track step between the maximum intensity and the radius of the cyclone shown in Figure 4b, the number of cyclones that reach both at the same time accounts for 45% of the total number of cyclones. Of the remaining Jianghuai cyclones, more reach the maximum intensity first and continue to develop to the maximum horizontal scale.
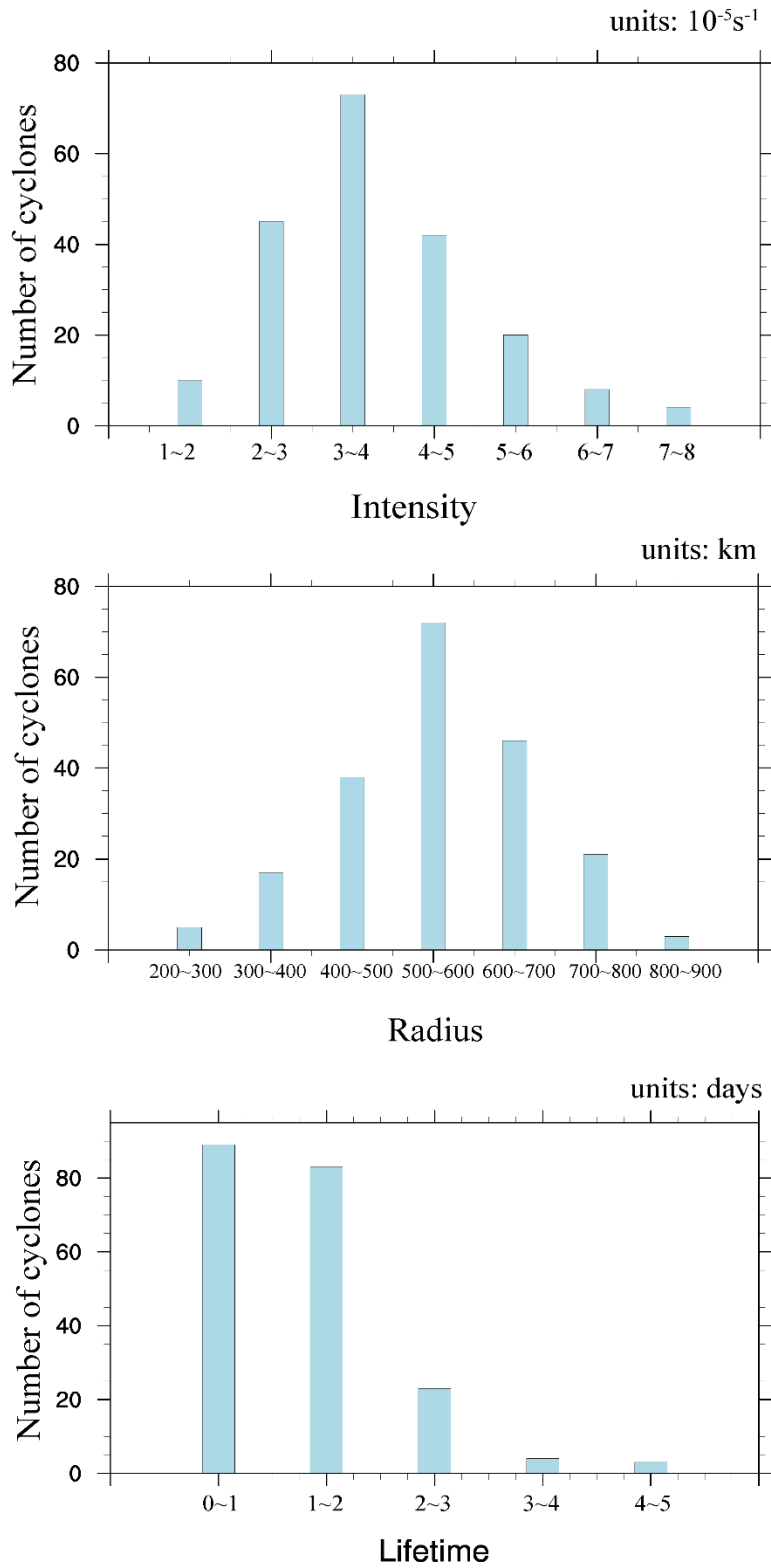
224    Fig 3. Distributions of the number of selected cyclones versus their (a) intensities (units:

225    $10^{-5}$ s$^{-1}$), (b) radii (units: km), and (c) lifetimes (units: days).
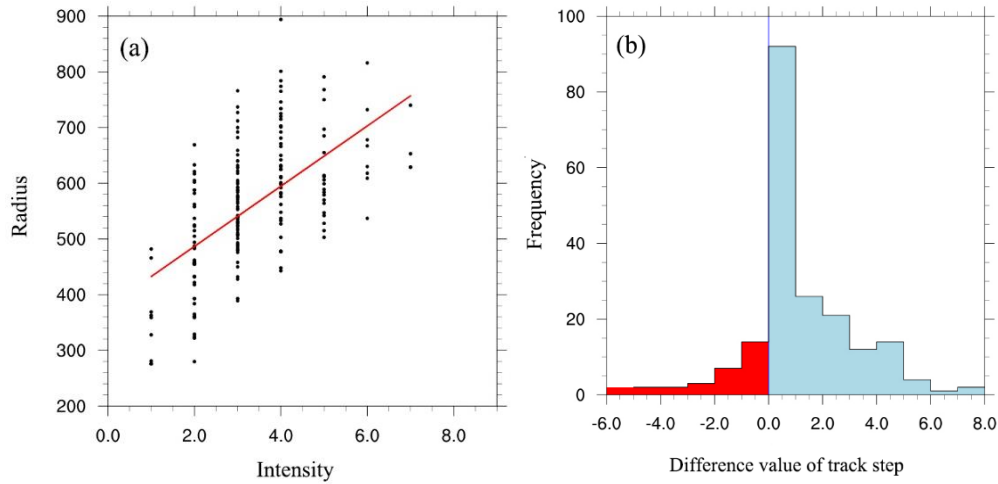
Fig 4. Correlation between maximum intensity (units: $10^{-5}$ s$^{-1}$) and maximum radius (units: km) (a) and their difference value of track step during the development of the Jianghuai cyclone in the Meiyu period (b).

The frequency of Jianghuai cyclone occurrence refers to the total number of cyclones is characterized by quasi-periodic variation (Figure 5). The shaded area in the figure indicates that the 95% confidence interval according to Student's t-test is passed. Strong 2~4 years quasiperiodic variation is observed for 1980-1990 and 1990-2000. After 2000, the quasiperiodic change in cyclones is approximately 4~5 years. This change period corresponds to the period of abnormal change in Meiyu. Chen et al. (2019) pointed out that 3~4 years of quasiperiodic change is the main component of abnormal changes in Meiyu when studying the quasiperiodic change in Meiyu. This quasi-periodic variation component is mainly influenced by the Indian Ocean dipole (IOD) (Liang et al., 2018). During the positive phase of the IOD, the strong warming of the Indian Ocean triggers a strong Indian monsoon. This leads to a strengthening of the WPSH and an increase in precipitation in southern China. The southwesterly low-level jet, which are enhanced by the positive IOD, also provide water vapor and warm advection to generate favorable conditions for the development of the Jianghuai cyclone.
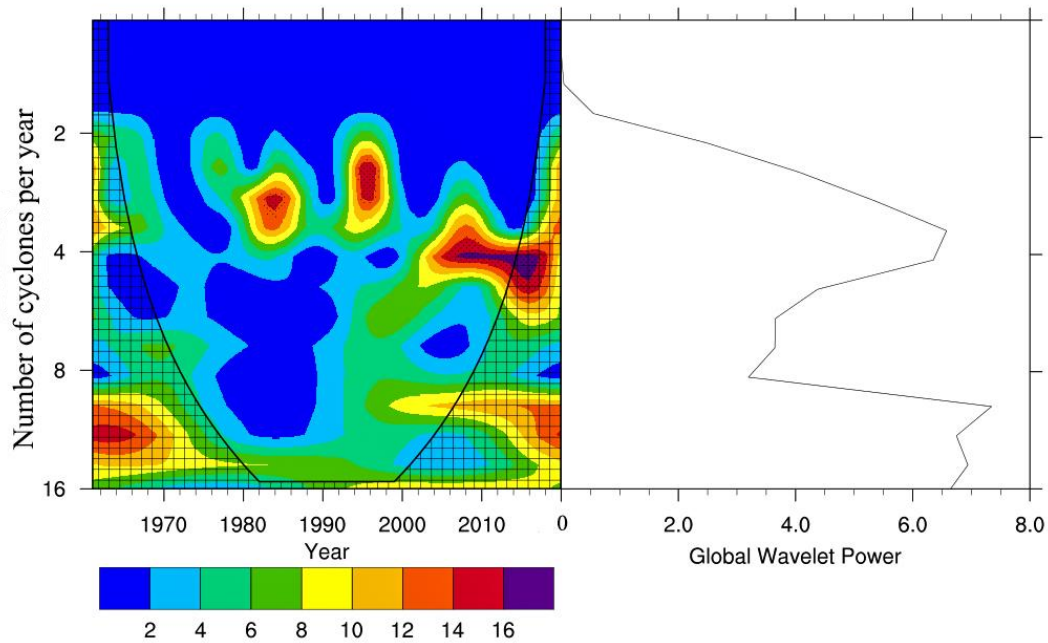
243     Fig 5. Periodic wavelet analysis diagram of Jianghuai cyclones during the Meiyu period

244     from 1961 to 2020 (units: year) (shadow indicates passing the 95% confidence interval

245     according to Student's t-test).

246        Jianghuai cyclones are not only characterized by quasi-periodic variation but also

247     have significant decadal variation. Figure 6 shows the activity frequency anomaly and

248     5-year sliding average of cyclones during the Meiyu period from 1961 to 2020. The

249     frequency of cyclone activity was the highest in 1996 and the lowest in 1961 and 2009.

250     In the long term, the frequency of cyclone activity in the middle and lower reaches of

251     the Yangtze River with positive anomaly in 1965-1970, 1990-2000, and 2000-after, and

252     negative anomaly in 1970-1990 and 2000-2010. The decadal variation trend of

253     Jianghuai cyclones is similar to the decadal variation of precipitation during the Meiyu

254     period (Chen et al., 2019). The decadal variation of precipitation during the Meiyu

255     period with positive anomaly in 1965-1970, 1995-2000 and 2010-after, and negative

256     anomaly in 1970-1980, 1985-1995 and 2000-2010.
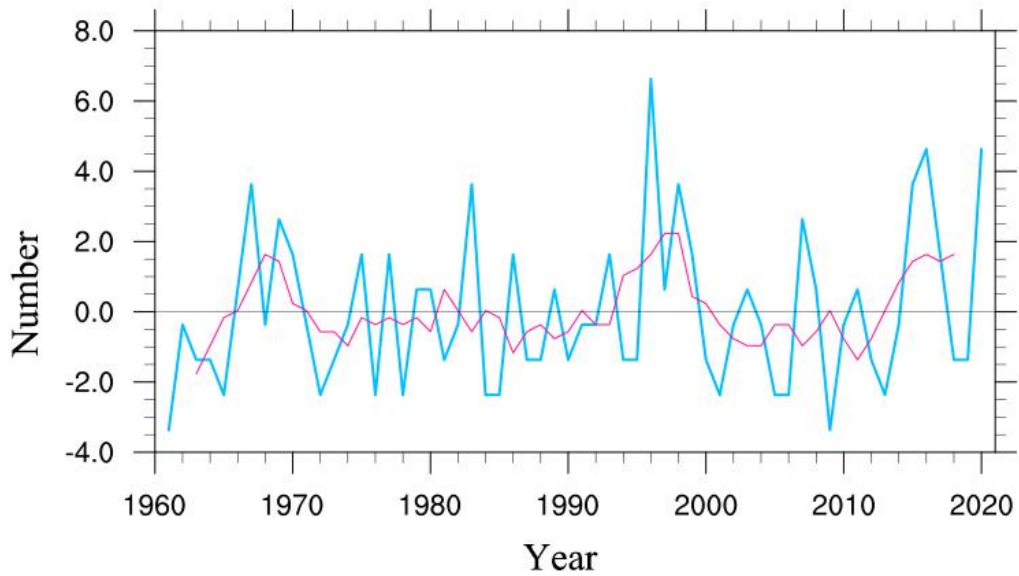
257    Fig 6. Frequency anomaly and 5-year sliding average of cyclones. The blue line shows

258    the anomalies in the number of cyclones, and the pink line shows the 5-year sliding

259    average of the anomalies.

260    **3.2 Linkage between cyclone activity and concurrent rainfall in the middle and**

261    **lower reaches of the Yangtze River.**

262    The Jianghuai cyclones are mainly active in the middle and lower reaches of the

263    Yangtze River (Huang et al., 2019; Li et al., 2002). Under the influence of the

264    strengthening westward extension of the WPSH during the Meiyu period, the Jianghuai

265    cyclones are restricted from entering the sea to some extent (Qin et al., 2015; Wu et al.,

266    2020b). They form rainstorms in the middle and lower reaches of the Yangtze River and

267    the coastal areas. A large part of the precipitation in the Meiyu period comes from

268    cyclone precipitation (Zhang et al., 2018). The intensity of Meiyu is usually expressed

269    by the Meiyu intensity index. The intensity of precipitation is affected not only by

270    precipitation but also by the number of precipitation days in the Meiyu period. Both

271    jointly determine the intensity of Meiyu in that year.

272    The time-series plots of the number of cyclones related to precipitation and the

273    intensity index during the Meiyu period from 1961 to 2020 are given in Figure 7a and

274    7b. We found that the number of cyclones has a positive correlation coefficient of 0.77

with precipitation in the Meiyu period passing the 99% confidence interval according to the student's t-test. The number of cyclones was also positively correlated with the Meiyu intensity index, with a correlation index of 0.76 passing the 99% confidence interval according to the student's t-test.
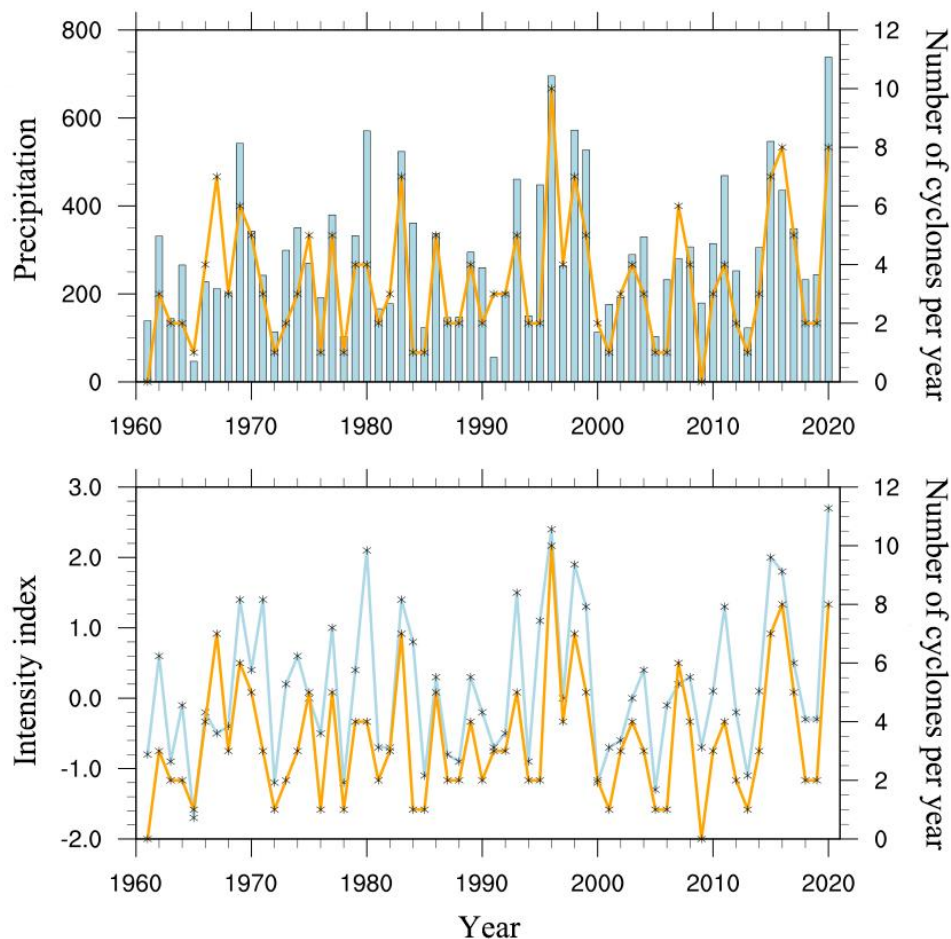
Fig 7. (a) Changes in precipitation (blue bar chart) (unit: mm/day) and the number of cyclones (orange line); (b) intensity index (blue line) and the number of cyclones (orange line) in the Meiyu period from 1961 to 2020.

Figure 8a shows the spatial distribution of mean annual total precipitation during the Meiyu period from 1961 to 2020. The areas with large precipitation values in the middle and lower reaches of the Yangtze River are mainly located in the Dabie Mountains of Anhui Province, the northern part of Jiangxi Province, the eastern part of Hubei Province and the western part of Hubei Province. The maximum annual average

precipitation during the Meiyu period in southern Anhui can even exceed 480 mm. The occurrence of large precipitation areas during the Meiyu period is closely related to the topography of the region (Wu et al., 2023).

If precipitation and Jianghuai cyclone activity existed on the same day during the Meiyu period, we defined that day as a Jianghuai cyclone precipitation day. Figure 8b shows the spatial distribution of the proportion of cyclone precipitation relative to total precipitation during the Meiyu period. As shown in the figure, the main areas affected by cyclone precipitation are the middle and lower reaches of the Yangtze River. The Huaihe River basin in northern Anhui Province is the most affected area. The cyclone precipitation in the Huaihe River basin accounts for more than 47% of the total precipitation during the Meiyu period, while the cyclone-influenced precipitation in other areas accounts for more than 35% of the total precipitation. In general, the degree of cyclone-influenced precipitation in the middle and lower reaches of the Yangtze River shows an east–west band distribution and a gradual decrease from coastal to inland areas. This indicates that the distribution of the large-value area and the characteristics of the band distribution are related to the northeast and eastward tracks of the Jianghuai cyclone. Its precipitation capacity gradually increases with the development of cyclone movement.

Figure 8c shows the spatial distribution of the daily mean precipitation anomaly of the Jianghuai cyclone. The shaded part indicates that the 95% confidence interval is passed according to Student's t-test. The anomalies mentioned here and later are the difference between the daily mean value of meteorological elements of the selected Jianghuai cyclones and the corresponding daily mean value of sixty years. When the Jianghuai cyclone is active, the middle and lower reaches of the Yangtze River to the east of 108°E show an abnormal increase in precipitation. However, Fujian, Guangdong and other places show an abnormal decrease. Among them, the maximum value of abnormally increased precipitation can exceed 7 mm/day in areas such as southern Anhui, eastern Hubei and northern Jiangxi. The large-value areas of precipitation anomalies are consistent with the large-value areas of cyclone occurrence frequency

sources. It is inferred that the spatial distribution of precipitation anomalies has a connection with the distribution of cyclone genesis locations. This phenomenon of increasing and decreasing precipitation anomalies is bounded by approximately 27°N and distributed north–south in the form of dipoles.
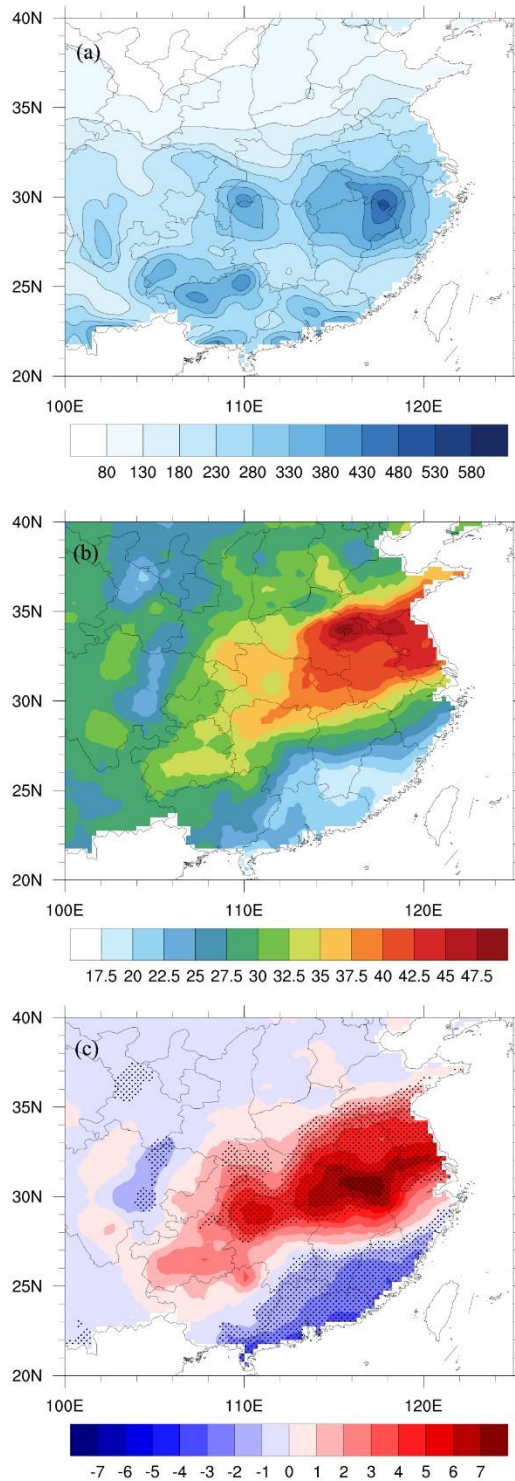
Fig 8. (a) Mean annual total precipitation during the Meiyu period from 1961 to 2020

321 (units: mm/year); (b) proportion of Jianghuai cyclone precipitation relative to total

322 precipitation during the Meiyu period (units: %); (c) daily mean precipitation anomaly

323 of the Jianghuai cyclone during the Meiyu period (units: mm/day) (shadow indicates

324 passing the 95% confidence interval according to Student's t-test).

325 Figure 9 shows the evolution of composite geopotential height and horizontal wind

326 anomalies for two different levels of Jianghuai cyclones from day -4 to +2 during the

327 Meiyu period. Composite geopotential height anomalies are significant at the 95%

328 confidence level based on Student's t-test. Vectors are plotted if wind anomalies are

329 significant at the 95% confidence level based on Student's t-test in at least one direction.

330 Day 0 is the day on which the cyclone first appears in the specified area. Most

331 areas of the lower and middle troposphere (850 hPa) in the middle and lower Yangtze

332 River on day 0 are covered by significant negative geopotential height anomalies with

333 peak magnitudes greater than -11 gpm. There is a significant positive geopotential

334 height anomaly with a peak magnitude of over 13 gpm on the southeast side of the

335 negative geopotential height anomaly. These anomalies form meridional dipole

336 structures in the middle and lower troposphere geopotential height field. The southwest

337 wind anomaly is significant in the middle and lower reaches of the Yangtze River. The

338 south of Anhui Province and the north of Jiangxi Province are between the positive

339 geopotential height anomaly and negative geopotential height anomaly. The existence

340 of these anomalies indicates the enhancement of southwest rapids and the strengthening

341 of the WPSH. The negative geopotential height anomalies at 500 hPa height on day 0

342 are mainly in Mongolia, Shanxi and other places. Strong southwest wind anomalies

343 exist between the positive and negative geopotential height anomalies. The negative

344 geopotential height anomalies in the Mongolian region exceed -7 gpm.

345 The negative geopotential height anomalies on all three isobaric surfaces can be

346 traced back to Mongolia, Inner Mongolia and part of Northeast China on day -2.

347 Negative geopotential height anomalies at 500 hPa can be traced to day -4. On day -4,

348 significant southwestern wind anomalies exist in southwestern Hunan at 850 hPa.

Significant northwest wind anomalies exist in the Yellow River basin of China at 500 hPa. By day -2, the negative geopotential height anomalies in Mongolia, Inner Mongolia and some northeastern areas are enhanced for all three isobars. The positive geopotential height anomalies of the WPSH are enhanced and extend northward to the southern part of the middle and lower reaches of the Yangtze River. There are significant southwest wind anomalies at the three isobaric surfaces in the south of the middle and lower reaches of the Yangtze River, while there are significant northwest wind anomalies at 500 hPa in the north of Anhui Province and Jiangsu Province. The negative geopotential height anomalies on the three isobaric surfaces move eastward with the formation and development of Jianghuai cyclones. On day +2, the lower reaches of the Yangtze River are mainly affected by the combined action of anomalous southwest winds and northwest winds. The positive geopotential height anomaly of the WPSH is weakened.

Therefore, the abnormal precipitation caused by the Jianghuai cyclone mainly comes from the abnormal southwest winds and the strengthening of the WPSH. The enhanced southwesterly low-level jet provides sufficient warm and moist air for the formation of cyclones and promotes the eastward migration of cyclones after formation. Liu et al. (2020) and Zhao et al. (2021) studied the causes of the super strong Meiyu year in 2020, mentioned that the WPSH is unusually strong and westward accompanied by an abnormal increase in precipitation. Liu et al. (2020) found that the enhanced the southwesterly low-level jet stream is conducive to the development of vertical movement in the middle and low levels, which provides the necessary dynamic conditions for the formation of sustained precipitation during the Meiyu in 2020.

Cold air activity is one of the important factors for the formation of heavy precipitation, which can promote the convergence and uplift of low level necessary for heavy precipitation (Liu et al., 2020). The enhanced negative geopotential anomaly over Mongolia provides cold and dry air brought by the westerly jet for cyclone development. The increasing frequency of cyclones over the Yangtze River and Huaihe River leads to the abnormal increase in precipitation in the middle and lower reaches of

378 the Yangtze River during the Meiyu period. However, due to the strengthening of the

379 WPSH, the southern part of China is controlled by the abnormal positive geopotential

380 height, and the precipitation decreases. Zhao et al. (2021) also found that when the

381 WPSH enhanced, there was a decrease in precipitation in South China.
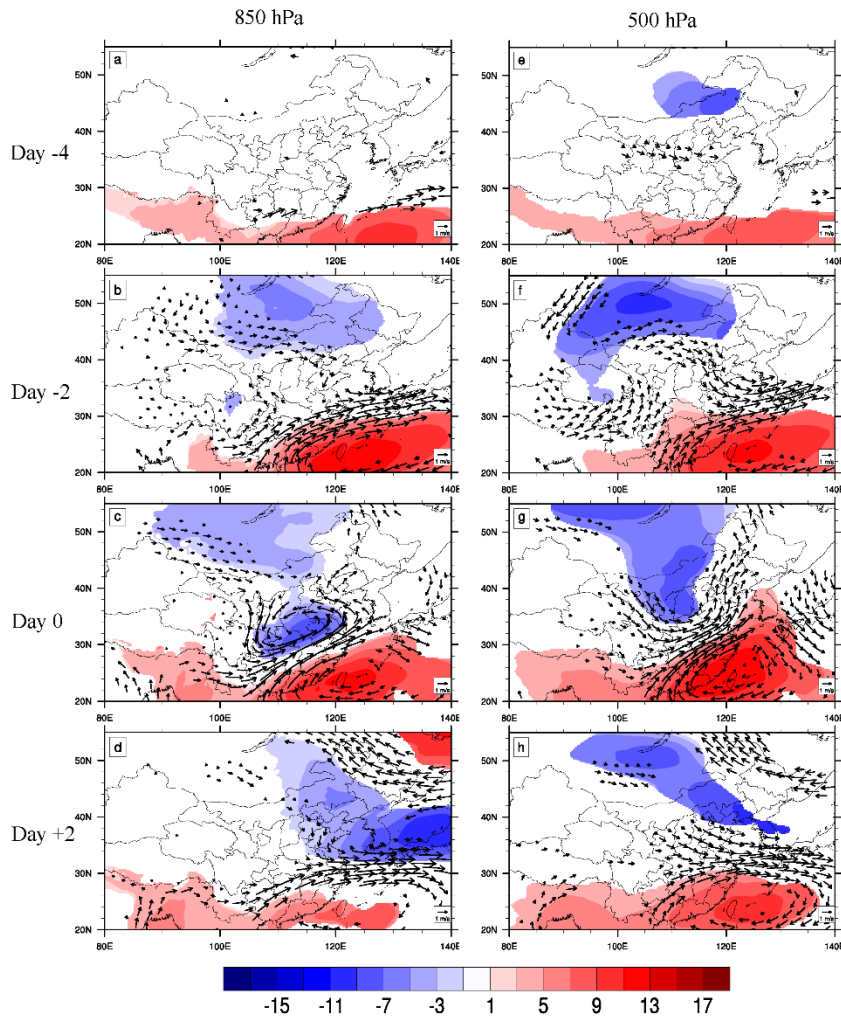
382 Fig 9. Evolution of composite geopotential height anomalies (shading; units: gpm) and

383 horizontal wind anomalies (units: m/s) on the 850 hPa and 500 hPa isobaric surfaces

384 for day −4 (a, e), day −2 (b, f), day 0 (c, g) and day +2 (d, h) for the 202 selected

385 Jianghuai cyclones. Shading indicates that composite geopotential height anomalies are

386 significant at the 95% confidence level based on Student's t-test. Vectors are plotted if

387 wind anomalies are significant at the 95% confidence level based on Student's t-test in

388 at least one direction.

389  Figure 10 shows the climatic distribution of water vapor flux and water vapor flux

390    divergence at 850 hPa of Jianghuai cyclone during the Meiyu period. The water vapor

391    involved in the precipitation process of the Jianghuai cyclone mainly comes from the

392    water vapor brought by the southwesterly low-level jet of the summer monsoon in the

393    low-latitude area. During Jianghuai cyclone development, the middle and lower reaches

394    of the Yangtze River are mostly in the water vapor convergence area, which is

395    conducive to the generation of precipitation (Chen et al., 2020).

396    Figure 11 shows the distribution of water vapor flux anomalies and water vapor

397    flux divergence anomalies at the pressure level of 850 hPa during the Jianghuai cyclone

398    from day -1 to day +2. The color field and wind vector arrows in the figure both passed

399    the 95% significance according to Student's t-test. On day -1, a significant water vapor

400    convergence anomaly and water vapor transport in the southwest direction appear in

401    eastern and western Hubei Province. In the middle reaches of the Yangtze River, there

402    is a north-south distribution of water vapor convergence and divergence dipoles. The

403    anomalies of water vapor flux and water vapor flux dispersion are mainly concentrated

404    on day 0. There is significant anomalous water vapor convergence up to -1 $g \cdot cm^{-2} \cdot hPa^{-1}$

405    in eastern Hubei Province, Anhui Province and Jiangsu Province on day 0. Anomalous

406    water vapor dispersion exists in the middle and lower reaches of the Yangtze River. On

407    the day +1 of cyclone development, the spatial distribution of water vapor convergence

408    and divergence shifted to an east-west direction. The anomalous transport of water

409    vapor flux also changes to an east-west direction. On day +2, with the development of

410    the cyclone's eastward movement, only the southern part of Jiangsu Province and the

411    northern part of Zhejiang Province have abnormal water vapor flux in the eastward

412    direction. The precipitation in the area begins to gradually weaken at this time.

413    From day -1 to day 0, the abnormal water vapor flux and water vapor flux

414    divergence configuration make the warm and wet air in the low-latitude area transport

415    to the middle and lower reaches of the Yangtze River. The abnormal water vapor flux

416    has a negative value, water vapor convergence occurs, local water vapor volume

417    increases, and finally, the precipitation in the region increases. Liu et al. (2020) studied

418    the strong rainfall in 2020, they found that there was an enhanced water vapor transport,

419 and the repeated occurrence of convergence movement. Both of them caused the

420 precipitation time to increase in the Jianghuai River basin.

421     In contrast, the anomaly of water vapor flux in southern Guangdong and other

422 regions is divergent. This leads to a decrease in local water vapor volume and

423 precipitation in this region. These results indicate that the variations in water vapor flux

424 and divergence related to cyclones are mainly from warm and wet air transported from

425 low latitudes to the middle and lower reaches of the Yangtze River. Therefore, there is

426 a positive correlation between cyclone activity and precipitation in the middle and

427 lower reaches of the Yangtze River.
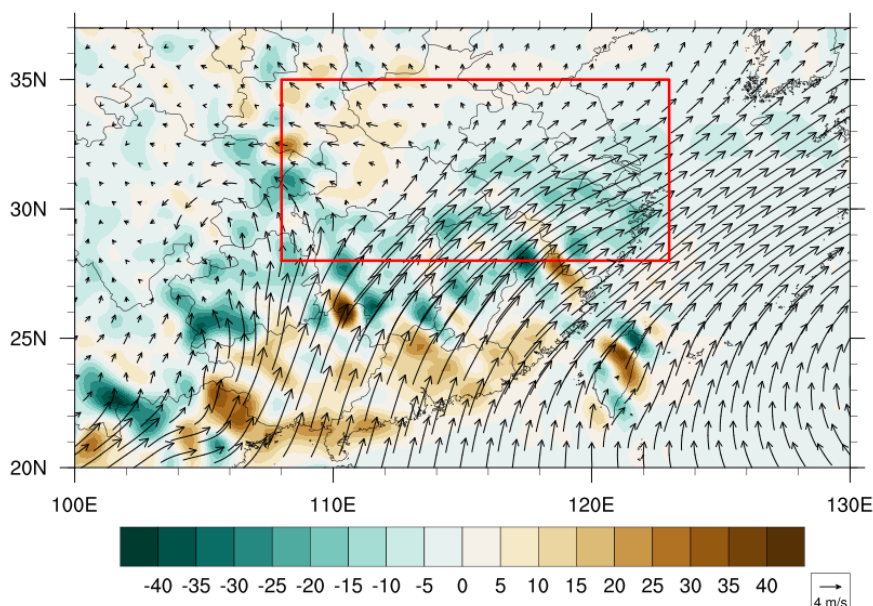
428 Fig 10. Distribution of 850 hPa daily mean water vapor flux (unit: $g \cdot cm^{-2} \cdot hPa^{-1}$) and

429 water vapor flux divergence (unit: $10^{-8}$ $g \cdot cm^{-2} \cdot hPa^{-1} \cdot s^{-1}$) of cyclones over the Yangtze

430 and Huaihe rivers during 1961-2020 (color diagram shows water vapor flux divergence,

431 and vector diagram shows water vapor flux).
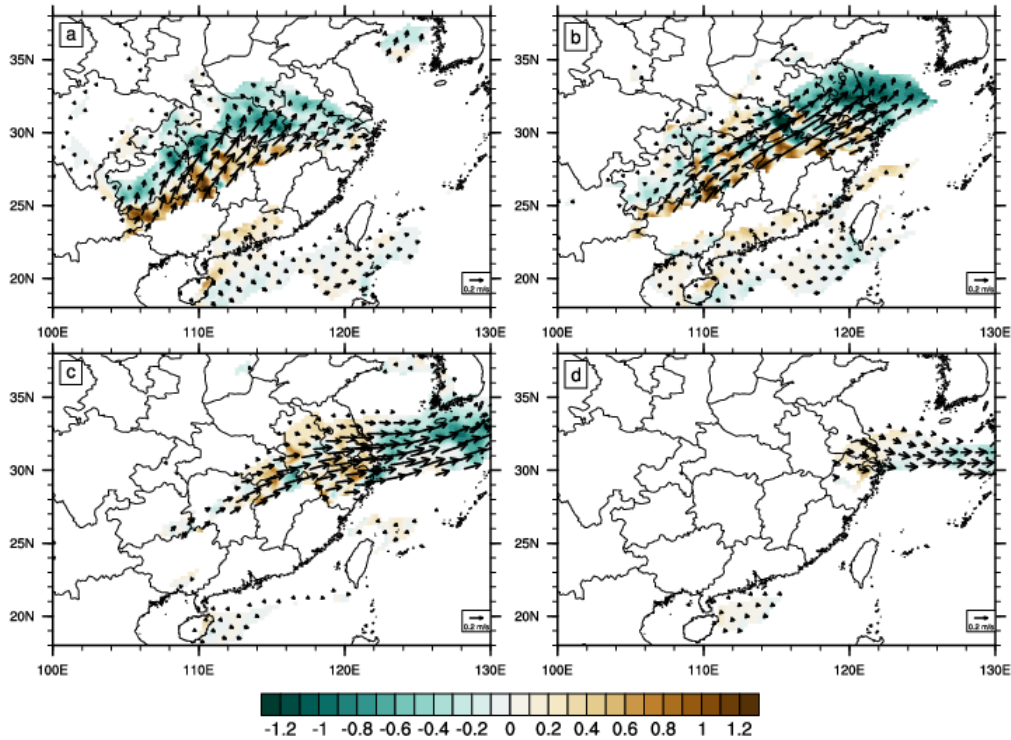
Fig 11. Distribution of the 850 hPa daily mean water vapor flux anomaly (unit: $g \cdot cm^{-2} \cdot hPa^{-1}$) and water vapor flux divergence anomaly (unit: $10^{-8}$ $g \cdot cm^{-2} \cdot hPa^{-1} \cdot s^{-1}$) of cyclones over the Yangtze and Huaihe rivers during 1961-2020 (color diagram shows water vapor flux divergence, and vector diagram shows water vapor flux). The colored region passed the 95% confidence interval according to Student's t-test. If the vapor flux anomaly is significant at the 95% confidence level for Student's t-test in at least one direction (zonal or meridian), the vector is plotted.

## 4. Summary and discussion

Based on ERA5 reanalysis of sea level pressure data and using the relative vorticity method to identify and track cyclones, we have examined the impacts of the climatological characteristics of Jianghuai cyclones. The linkages between cyclone activity and precipitation in the middle and lower reaches of the Yangtze River during the Meiyu period are also analyzed.

During the Meiyu period, Jianghuai cyclones are mainly generated at the junction of western Hubei and Chongqing Municipality, eastern Hubei Province, northern

447 Jiangxi Province, central and southern Anhui Province, and Jiangsu and Zhejiang

448 provinces. These cyclones develop and move to the sea in the east or northeast direction.

449 There is a positive correlation between the maximum intensity and maximum radius of

450 Jianghuai cyclones. Its occurrence frequency not only has the characteristics of

451 multicycle variation but also has obvious interdecadal variation, which has a good

452 correspondence with the periodic and interdecadal variation in precipitation in the

453 Meiyu period.

454     There is a positive correlation between the frequency of cyclone activity and

455 precipitation in the Meiyu period. The frequency of Jianghuai cyclone activity is high

456 in the years with strong Meiyu rainfall and low in the years with weak Meiyu rainfall.

457 The percentage of precipitation affected by Jianghuai cyclone activity in the middle and

458 lower reaches of the Yangtze River can reach up to 47%. The spatial distribution is in

459 the shape of an east–west belt, and the degree of influence gradually decreases from the

460 coast to the interior. When the Jianghuai cyclone is active, the precipitation increases

461 abnormally in the middle and lower reaches of the Yangtze River east of 108°E.

462 Precipitation decreases abnormally in Fujian Province and Guangdong Province. The

463 spatial distribution of precipitation anomalies is related to the genesis locations of

464 cyclone frequency, and the positive and negative anomalies are distributed north–south

465 in the form of dipoles based on the latitude line at approximately 27°N as the boundary.

466     The geopotential height anomaly field and the horizontal wind vector anomaly

467 field of the Jianghuai cyclones during the Meiyu period are synthesized and analyzed.

468 There is an enhanced positive geopotential height anomaly of the WPSH during cyclone

469 activity. The negative geopotential altitude anomaly of Mongolia and the abnormal

470 southwesterly low-level jet are enhanced. All of these factors lead to an increase in

471 precipitation in the middle and lower reaches of the Yangtze River. The abnormal

472 leading signal of the negative geopotential height in Mongolia can be traced to day -2

473 of the cyclone activity, and the signal can be traced to day -4 at 500 hPa. From day -2

474 to day 0 of cyclone activity, the abnormal distribution of water vapor flux and water

475 vapor flux divergence cause the warm and wet air at the low latitudes to be transported

to the middle and lower reaches of the Yangtze River. They promote the generation and development of cyclones and increase precipitation in the middle and lower reaches of the Yangtze River.

We explored the cyclone characteristics and study emphasizes the link between cyclone activity and Yangtze River precipitation. Spatially, abnormal precipitation patterns are identified, tracing the evolution of geopotential height anomalies and water vapor flux. But the specific mechanism by which the southwesterly low-level jet affects cyclones during the Meiyu period is not clear enough. Zhang et al. (2018) suggest that the strengthening of the southwesterly low-level jet will lead to the development of α mesoscale low-pressure disturbance near the Meiyu Front and the occurrence of extreme precipitation. Liu et al. (2020) found that the strengthening of the southwesterly low-level made the southerly meridional strong gradient zone on the north side of the meridional wind maximum center move northward in the low-level dynamic conditions of the rainstorm process during Meiyu. How the southwesterly low-level stream influences the development of physical factors to promote the formation of Jianghuai cyclones remains to be considered and analyzed. Zhao et al. (2010) found that the causes of Jianghuai cyclones with different intensities were different through a case study. Therefore, we think it is also necessary to consider the difference in the influence of different intensities of Jianghuai cyclones on precipitation. These problems need further analysis and research.

**Competing interests**

The contact author has declared that none of the authors has any competing interests.

**References**

Bao, Y, Y.: Similarities and Differences of Monsoon Circulations between 2016 and 1998 Meiyu Periods in Middle and Lower Reaches of the Yangtze River and Comparison of Their Physical Mechanisms. Chinese Journal of Atmospheric Sciences., 45, 994−1006, 2021. DOI: 10.3878/j.issn.1006-9895.2101.20174

Cai, Y, X., He, H., Lu, H., Zhu, L, Y., and Lu, Q, Q.: Synoptic and climatic characteristics of persistent rainstorm in Guangxi in June 2020. Journal of Meteorological Research and Application., 4, 113-117, 2021. DOI:10.19849/j.cnki.CN45-1356/P.2021.1.20.

Chen, L, J., Zhao, J, H., Gu, W., Liang, P., Zhi, R., Peng, J, B., Zhao, S, Y., Gao, H., Li, X. and Zhang, P, Q.: Advances of Research and Application on Major Rainy Seasons in China. Journal Of Applied Meteorological Science., 30, 385-400, 2019. DOI: 10.11898/1001-7313.20190401

Chen, T., Zhang, F, H., Yu, C., Ma, J., Zhang, X, D., Shen, X, L., Zhang, F. and Luo, Q.: Synoptic analysis of extreme Meiyu precipitation over Yangtze River Basin duing June-July. Meteor Mon., 46, 1415-1426, 2020. DOI: 10.7519/j.issn.1000-0526.2020.11.003

Ding, Y, H.: Summer monsoon rainfalls in China. J Meteor Soc Jpn.,70, 373-396, 1992. DOI: https://doi.org/10.2151/jmsj1965.70.1B_373

Ding, Y, H.: Seasonal march of the east-Asian summer monsoon. Chang C P. East Asian Monsoon. Hackensack: World Scientific., 64, 2004. DOI: https://doi.org/10.1142/9789812701411_0001

Ding, Y, H., Liu, J, J., Sun, Y., Liu, Y, J., He, J, H., Song, Y, F.: A Study of the Synoptic-Climatology of the Meiyu System in East Asia. China J Atmos Sci., 31, 1082-1101, 2007. DOI: https://d.wanfangdata.com.cn/periodical/daqikx200706006

General Administration of Quality Supervision, Inspection and Quarantine of the People's Republic of China, Standardization Administration of the People's Republic of China. GB/T 33671-2017, Meiyu monitoring indices. DOI:http://fj.cma.gov.cn/zfxxgk/zwgk/flfgbz/dfbz/202209/t20220921_5098384.htm

527    l

He, L, F., Chen, T., Zhou, Q, L. and Li, Z, C.: The Meso-β Scale Convective System of
    a Heavy Rain Event on July 10, 2004 in Beijing. Journal Of Applied Meteorological
    Science., 18, 655-665, 2007. DOI: 10.3969/j.issn.1001-7313.2007.05.010

Hersbach, H., and Coauthors.: ERA5 hourly data on pressure levels from 1940 to
    present. Copernicus Climate Change Service (C3S) Climate Data Store (CDS)., 2018.
    DOI: 10.24381/cds.bd0915c6

Hodges, K. I.: A general method for tracking analysis and its application to
    meteorological data. Monthly Weather Review., 122, 2573-2586, 1994.
    DOI:https://doi.org/10.1175/1520-0493(1994)122<2573:AGMFTA>2.0.CO;2.

Hodges, K, I.: Feature tracking on the unit sphere. Monthly Weather Review., 123,
    3458-3465, 1995.
    DOI:https://doi.org/10.1175/1520-0493(1995)123<3458:FTOTUS>2.0.CO;2.

Huang, W, Y., Sun, Y., Lu, C, H., Yao, L, N. and Dong, Q.: Statical analysis of Jianghuai
    cyclone causing Jiangsu regional heavy rain in summer nearly 40 years. Meteor Mon.,
    45, 843-853, 2019.DOI: 10.7519/j.issn.1000-0526.2019.06.010

Jiang, L, Z., Fu, S, M., Sun, J, H.: New method for detecting extratropical cyclones: the
    eight-section slope detecting method. Atmospheric and Oceanic Science Letters, 13,
    436-442, 2020.
    DOI:10.1080/16742834.2020.1754124.

Jiangsu Provincial Weather Bureau: Jiangsu Provience Weather Forecast Techniacal
    Manual. Beijing: China Meteorological Press., 22-33, 2017.

Li, B., Yu, W, P., Lu, Y. and Lu, D, C.: The numerical simulating study of the mesoscale
    characteristics on development of Jianghuai cyclones. Science meteorologic., 22, 72-
    80, 2002. DOI: 10.3969/j.issn.1009-0827.2002.01.009.

Liang, P., Chen, L, J., Ding, Y, H., He, J, H. and Zhou, B.: Relationship between long-
    term variability of Meiyu over the Yangtze River and ocean and Meiyu's
    predictability study. Acta Meteorologica Sinica., 76, 379-393, 2018.
    DOI:10.11676/qxxb2018.009.

Liu, Y, Y., Ding, Y, H.: Characteristics and possible causes for extreme Meiyu in 2020. Meteor Mon.,46, 1393-1404, 2020. DOI: 10.7519/j.issn.1000-0526.2020.11.001

Lu, C, H.: A Modified Algorithm for Identifying and Tracking Extratropical Cyclones. Advances in atmospheric sciences., 34, 909-924, 2017.DOI: 10.1007/s00376-017-6231-2

Pascal, J, Mailier., David, B, Stephenson., Christopher, A, T, Ferro.: Serial Clustering of Extratropical Cyclones. Monthly weather review, 134, 2224-2240, 2006.

Ninomiya, K., Murakami, T.: The early summer rainy season (Baiu) over Japan. Monsoon Meteorology., New York: Oxford University Press, 93-121, 1987.

Oh, T, H., Kwon, W, T., Ryoo, S, B.: Review of the researches on Changma and future observational study. Adv Atmos Sci, 14, 207-222, 1997.

Pang, Y., Wang, L, J. and Yu, B.: The relationship between 10-30d low frequency oscillation and the rainfall over Changjiang-Huaihe River valley during Meiyu period. Trans Atmos Sci., 36, 742-750, 2013.

DOI: 10.3969/j.issn.1674-7097.2013.06.011

Qian, W, H., Lee, D, K.: Seasonal march of Asian summer monsoon. Int J Climatol., 20, 1371-1386, 2000.

DOI: 10.1002/1097-0088(200009)20:11<1371::AID-JOC538>3.0.CO;2-V

Qin, T., Wei, L, X.: The statistic and variance of cyclones entering coastal waters of china in 1979-2012. Acta Oceanologica Sinica., 2015.

DOI: 10.3969/j.issn.0253-4193.2015.01.005

Saito, N.: Quasi-stationary waves in mid-latitudes and Baiu in Japan. J Meteor Soc, 63, 983-995, 1995.

Shen, Y., Sun, Y., Cai, N, H., Su, X. and Shi, D, W.: Analysis on the generation and evolution of a Jianghuai Cyclone responsible for extreme precipitation event. Meteor Mon.,45, 166-179, 2019. DOI: 10.7519/j.issn.1000-0526.2019.02.003

Simmonds, I., Keay, K.: Mean Southern Hemisphere extratropical cyclone behavior in the 40-year NCEP-NCAR reanalysis. J Climate., 13, 873-885, 2000.

DOI: 10.1175/1520-0442(2000)013<0873:MSHECB>2.0.CO;2

Simmonds, I., Murray, R, J.: Southern extratropical cyclone behavior in ECMWF analyses during the FROST special observing periods. Weather& Fore-casting., 14, 878-891, 1999.

DOI:10.1175/1520-0434(1999)014<0878:SECBIE>2.0.CO;2

Su, X., Kang, Z, M., Zhuang, X, R. and Chen, S, J.: Uncertainty analysis of heavy rain belt forecast during the 2020 Meiyu period. Meteor Mon., 47, 1336-1346, 2021. DOI: 10.7519/j.issn.1000-0526.2021.11.003.

Tao, S, Y., Ding, Y, H. and Zhou, X, P.: Study on heavy rain and severe convective weather. Chinese Journal of Atmospheric Sciences.1979.

Wang, J, H., Niu, D., Ren, S, Y., Miao, C, S. and Song, P.: Comparative Study On Development Of Different Deep Jianghuai Rivers Cyclones Entering the Sea and the Influence of Environmental Factors. Journal Of Tropical Meteorology., 31, 744-756, 2016. DOI: 10.16032/j.issn.1004-4965.2015.06.003.

Wang, Y, L., Wang, L, J.: Characteristics of southern cyclone activity and its influence on precipitation in Yangtze River Basin. Yangtze River., 43, 34-36,68, 2012. DOI: 10.3969/j.issn.1001-4179.2012.09.009.

Wang, Y, L., Guan, Z, Y., Jin, D, C. and Ke, D.: Climatic characteristics and interannual variations of cyclones over Changjiang-Huaihe River basin during late spring and early summer from 1980 to 2012. Trans Atmos Sci., 38, 354-361, 2015. DOI: 10.13878/j.cnki.dqkxxb.20130413010

Wang, L, J., Huang, Q, L., Li, Y. and Han, S, R.: Relationship between spatial inhomogeneous distribution of Meiyu rainfall over the Yangtze-Huaihe River Valley and previous SST. Trans Atmos Sci, 37, 313-322, 2014. DOI: 10.3969/j.issn.1674-7097.2014.03.008

Wei, J, S., Liu, J, Y., Sun, Y. and Xu, Y, C.: Climate characteristics of Jiang-Huai cyclone. J Meteor Sci, 33, 196-201, 2013. DOI: 10.3969/2012jms.0112

Wernli, H., Schwierz, C.: Surface cyclone in the ERA-40 dataset (1958-2001). Part I: Novel identification method and global climatology. J Atmos Sci., 63, 2486-2507, 2006.

Wu, J., Gao, X, J.: A gridded daily observation dataset over China region and comparison with the other datasets. Chinese Journal of Geophysics., 56(4), 1102-1111, 2013.

Wu, J, F., Xu, X, F., Zhao, W, R., Qing, Q. and Zou, L.: Characteristics of Persistent Heavy Rainfall and Water Vapor Transport in Western Sichuan Plateau. Meteorological science and technology., 48, 704-716, 2020a. DOI:10.19517/j.1671-6345.20190301.

Wu, Q., Chen, S, J., Bai, Y., Xia, L. and Wang, C, J.: Diagnostic analysis and numerical simulation of a heavy rainstorm associated with the Jianghuai cyclone. Journal of the Meteorological Sciences., 41, 86-98, 2021. DOI: 10.12306/2020jms.0029.

Wu, Q., Liu, T., Zhang, B., Zhang, Y. and Wang, Y.: A Comparative Analysis of the Heavy Rainstorm Processes of Two Jianghuai Cyclones. Anhui Agri, Sci, Bull., 26, 161-171, 2020b. DOI: 10.3969/j.issn.1007-7731.2020.09.058

Wu, Q., Feng, J, W., Wang, Y., Chen, Y. and Zhang, L, T.: Spatial and temporal distribution of cyclones over the Jianghuai River during 1979-2018. Meteorology of Shanxi., 06, 15-22, 2021. DOI: 10.3969/j.issn.1006-4354.2020.06.003

Wu, T., Xu, G, Y., Li, S, J. and Wei, F.: Characteristics and Causes of a Mixed-Type Convective Weather During the Formation and Development of a Jianghuai Cyclone in Spring. Advances in Meteorological Science and Technology., 48, 704-716, 2023. DOI:10.19517/j.1671-6345.20190301.

Xu, J., Zhou, C, Y. and Gao, T, C.: Analysis about Development Mechanism of Jianghuai Cyclone in Meiyu Front and Its Relationship with Rainstorm. Bulletin Of Science and Technology., 29, 24-29,86, 2013. DOI: 10.3969/j.issn.1001-7119.2013.05.006.

Xu, J, M.: Satellite Imagery Characteristics for Extratropical Cyclones and Meiyu Font. Advances in Meteorological Science and Technology., 11, 14-26, 2021. DOI: 10.3969/j.issn.2095-1973.2021.03.003

Xu, Y., Gao, X, J., Shen, Y., Xu, C, H., Shi, Y., Giorgi, F.: A daily temperature dataset over China and its application in validating a RCM simulation. Advances in

Atmospheric Sciences., 26(4), 763–772, 2009.

Xu, Y, C., Wei, J, S. and Zhu, W, J.: A numerical simulation and marine sensitive experiments of Jiang-Huai cyclone. J Meteor Sic., 31, 726-731, 2011.

DOI: 10.3969/j.issn.1009-0827.2011.06.008

Yan, J, R., Wang, W, J., Zhang, H. and Shi, D, W.: Analysis of two rainstorm and gale processes of Jianghuai cyclone in Jiangsu Province in 2019. Journal of Meteorological Research and Application., 42, 83-88, 2021.

DOI: 10.19849/j.cnki.CN45-1356/P.2021.2.16

Yang, Y, M., Gu, W, L., Zhao, R, L. and Liu, J.: The statical analysis of vortex during Meiyu season in the lower reaches of the Yangtze. Quarterly Journal of Applied Meteorology., 21, 11-18, 2010. DOI: 10.3969/j.issn.1001-7313.2010.01.002

Zhao, B, K., Wu, G, X. and Yao, X, P.: A diagnostic analysis of potential vorticity associated with development of a strong cyclone during the Meiyu period of 2003. Chinese Journal of Atmospheric Sciences., 32, 1241-1255, 2008.

Doi: 10.3878/j.issn.1006-9895.2008.06.02.

Zhao, B, k., Wan, R, J. and Lu, X, Q.: A Contrastive Analysis on the Causes of Strong and Weak Cyclones over Yangtze-Huaihe River Valleys during the Meiyu Period in Summer of 2003. Plateau Meteorology., 29, 309-320, 2010.

Zhao, J, H., Chen, L, J. and Wang, D, Q.: Characteristics and causes analysis of abnormal Meiyu in China in 2016. Chinese Journal of Atmospheric Sciences., 42, 1055-1066, 2018. DOI: 10.3878/j.issn.1006-9895.1708.17170

Zhao, J, H., Zhang, H., Zuo, J, Q., Xiong, K, G. and Chen, L, J.: What Drives the Super Strong Precipitation over the Yangtze–Huaihe River Basin in the Meiyu Period of 2020. Chinese Journal of Atmospheric Sciences., 45, 1433−1450, 2021.

Doi:10.3878/j.issn.1006-9895.2104.2101.

Zhang, X, L., Tao, S, Y. and Zhang, S, L.: Three Types of Heavy Rainstorms Associated with the Meiyu Front. Chinese Journal of Atmospheric Sciences, 28., 187-205, 2004.

doi: 10.3878/j.issn.1006-9895.2004.02.03

Zhang, X, L., Tao, S, Y. and Zhang, Q, Y.: An Analysis on Development of MESO-β

Convective System along Meiyu Front Associated with Flood in Wuhan in 20-21 July 1998, Journal of Applied Meteorological Science., 13, 385-397, 2002. DOI: 10.3969/j.issn.1001-7313.2002.04.001.

Zhang, X, H., Luo, J., Chen, X., Jin, L, L. and Qiu, X, M.: Formation and development mechanism of one cyclone over Changjiang-Huaihe River basin and diagnostic analysis of rainstorm. Meteor Mon., 42, 716-723, 2016.

DOI: 10.7519/j.issn.1000-0526.2016.06.007

Zhang, J, G., Wang, J., Wu, T., Zhou, J, L., Zhong, M., Wang, S, S., Huang, X, Y., Li, S, J., Han, F, R. and Wang, X, C.: Weather system types of extreme precipitation in the middle reaches of the Yangtze River. Torrential Rain and Disasters., 37, 14-23, 2018.

Doi: 10.3969/j.issn.1004-9045.2018.01.003

Zhang, Y, X., Ding, Y, H. and Li, Q, P.: Cyclogenesis Frequency Changes of Extratropical Cyclones in the Northern Hemisphere and East Asia Revealed by ERA40 Reanalysis Data. Meteor Mon., 38, 646-656, 2012.

Zhou, J, L., Zhang, J, G., Wu, T., Xu, G, Y., Liu, X, W., Wang, J. and Han, F, R.: Characteristics of the mesoscale weather system producing extreme rainstorm in boundary layer during the Meiyu front over the middle reaches of Yangtze River. Meteor Mon., 48, 1007-1019, 2022. DOI: 10.7519/j.issn.1000-0526.2022.052801

Zhong, Q, M., Ma, J., Wang, L.: Biweekly oscillation of the Meiyu-season precipitation in 2016 and 2020 over the Yangtze Huaihe River basin:A comparative analysis. Acta Meteorologic Sinica., 8, 235-25, 2023. DOI:10.11676/qxxb2023.20220075

Zhou, X, M., Zheng, Y, G.: Analysis of Environmental Conditions and Tornado Storm Features of Two Tornadoes in Jiangsu during the Meiyu Period in 2020. Advances in Meteorological Science and Technology., 10, 34-42, 2020.

DOI: 10.3969/j.issn.2095-1973.2020.06.008.

Zhou, Y.,Xia, L.: Statistical Research on Climatic Characteristics of Jianghuai Cyclones. Meteorological and Environmental Sciences., 40, 79-85, 2017.

DOI: 10. 16765/ j. cnki.1673-7148.2017.03.013

701    Zhu, M., Lu, H, C. and Yu, Z, H.: Study of Positive Feedback Mechanism for Meso-α

702    Scale Cyclone Growing on Meiyu Front. Chinese Journal of Atmospheric Sciences.,

703    22, 763-770, 1998. Doi: 10.3878/j.issn.1006-9895.1998.05.11